A near-bottom magnetic survey of the Mid-Atlantic Ridge axis at 26°N: Implications for the tectonic evolution of the TAG segment

Maurice A. Tivey and Hans Schouten
Department of Geology and Geophysics, Woods Hole Oceanographic Institution, Woods Hole, Massachusetts, USA

Martin C. Kleinrock
Department of Geology, Vanderbilt University, Nashville, Tennessee, USA

Received 9 May 2002; revised 20 November 2002; accepted 19 February 2003; published 27 May 2003.

[1] An extensive deep-tow magnetic survey of the TAG ridge segment on the Mid-Atlantic Ridge reveals new information about the relationship between the magnetic anomaly field and the TAG hydrothermal deposits. Results show the strongest magnetization is located over the neovolcanic axis and asymmetrically toward the western side of the central Brunhes anomaly. A well-defined linear magnetization low is located over the eastern rift valley wall of the TAG segment. The near-bottom data show no direct correlation between this crustal magnetization low and the hydrothermal deposits. The magnetization low is explained by crustal thinning caused by 4 km of horizontal extension along a normal fault. Previous observations and sampling indicate exposures of gabbros and dikes in the eastern rift valley wall, suggesting slip along a normal fault has revealed this crust. Modeling suggests the fault has been active since 0.35 ± 0.1 Ma at a horizontal slip rate of roughly half the spreading rate of 22 km/Myr. The TAG hydrothermal system is located on the hanging wall of this fault within 3 km of its termination. Over the past several hundred thousand years, movement on the detachment fault may have episodically increased the permeability of the hanging wall reactivating the overlying hydrothermal systems. Significant vents like TAG may be typically associated with hanging walls of long-term detachment faults near seafloor spreading centers. This would imply that it is the reactivation of permeability in the hanging wall related to repeated fault movement that controls the longevity of these hydrothermal systems. *INDEX TERMS:* 1517 Geomagnetism and Paleomagnetism: Magnetic anomaly modeling; 1550 Geomagnetism and Paleomagnetism: Spatial variations attributed to seafloor spreading (3005); 8135 Tectonophysics: Hydrothermal systems (8424); 9325 Information Related to Geographic Region: Atlantic Ocean; *KEYWORDS:* magnetization, faulting, oceanic crust, hydrothermal vents

Citation: Tivey, M. A., H. Schouten, and M. C. Kleinrock, A near-bottom magnetic survey of the Mid-Atlantic Ridge axis at 26°N: Implications for the tectonic evolution of the TAG segment, *J. Geophys. Res.*, *108*(B5), 2277, doi:10.1029/2002JB001967, 2003.

1. Introduction

[2] The Trans-Atlantic Geotraverse (TAG) region of the Mid-Atlantic Ridge (MAR), located at 26°08′N in the North Atlantic Ocean (Figures 1 and 2), is well known for its vigorously active hydrothermal vent field and surrounding region of relict hydrothermal deposits [*Rona*, 1973; *Scott et al.*, 1974b; *Rona et al.*, 1976]. The TAG ridge segment is also known for a distinctive sea surface magnetic anomaly signal that is present over the area [*McGregor et al.*, 1977; *Wooldridge et al.*, 1990, 1992; *Tivey et al.*, 1993] (Figure 2b). Early sea surface magnetic surveys over the MAR revealed that a magnetic anomaly low within the central Brunhes anomaly was associated with the TAG ridge segment [*McGregor et al.*, 1977]. *McGregor et al.* [1977] modeled the magnetic low region as a zone of reduced magnetization using magnetic anomaly profiles. Their hypothesis was that crustal magnetization at the rift valley walls was reduced by hydrothermal alteration associated with a low-temperature hydrothermal field discovered on the eastern rift valley wall [*Scott et al.*, 1974a]. *McGregor et al.* [1977] found no evidence that block rotation of the rift valley walls could account for the observed magnetic anomaly lows. In 1985, a significant active high-temperature hydrothermal black smoker complex was discovered on the eastern side of the rift valley floor, at the base of the eastern wall [*Rona et al.*, 1984; *Thompson et al.*, 1985; *Rona et al.*, 1986b; *Thompson et al.*, 1988]. This presently active hydrothermal mound (i.e., the active TAG mound) is now known to form part of a larger hydrothermal field, which contains many relict hydrothermal deposits [*Lisitsyn et al.*, 1989; *Zonenshain et al.*, 1989; *Rona et al.*, 1993a, 1993b]. These discoveries renewed interest in the hydrothermal aspects of crustal demagnetization as a

0148-0227/03/2002JB001967$09.00

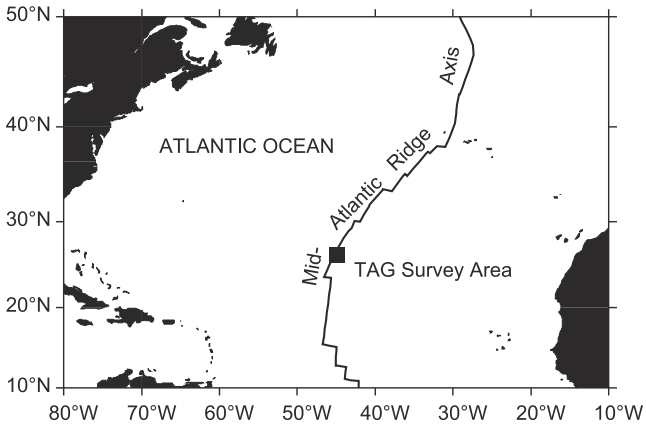

Figure 1. Location map showing location of TAG hydrothermal field located at 26°8′N, 44°49.5′W on Mid-Atlantic Ridge between the Kane and Atlantis fracture zones.

cause for the anomalous magnetic signal. *Wooldridge et al.* [1992] used three-dimensional inversion techniques [e.g., *Macdonald et al.*, 1980; *Parker and Huestis*, 1974] to reprocess the original 1972 sea surface magnetic field data and found an elongate region of low magnetization with its minimum centered on the active TAG hydrothermal mound. The data set, however, suffered from navigational uncertainties associated with the sporadic transit satellite coverage of that era. Subsequent surveys improved on this navigational uncertainty by using the global positioning satellite (GPS) system and in 1990 detailed swath bathymetry and high-resolution sea surface magnetic data were collected over the MAR between the Kane and Atlantis fracture zones [*Purdy et al.*, 1989]. These data further defined the elongate zone of reduced magnetization, but in contrast with the *Wooldridge et al.* [1992] analysis, the minimum was located several kilometers northeast of the TAG hydrothermal mounds [*Tivey et al.*, 1993]. This observation suggested that processes other than those associated with the active venting were responsible for the magnetic low [*Tivey et al.*, 1993]. The *Purdy et al.* [1989] data only covered the axial region of the MAR and so in the present analysis we have added sea surface magnetic field data from a survey of MAR west flank collected in 1992 [*Tivey and Tucholke*, 1998] and a similar survey of the eastern flank collected in 1996 (B. E. Tucholke and J. Lin, personal communication, 2002) (Figure 2b). An inversion of these combined data confirm the elongate magnetization low and the location of a magnetization minimum several kilometers to the northeast of the TAG hydrothermal mounds (Figures 2c and 2d).

[3] In addition to sea surface magnetic surveys, high-resolution near-bottom magnetic profiles were obtained using the deep submersible *Alvin* in a near-bottom draped survey over the active TAG mound [*Tivey et al.*, 1993]. This survey found a very short-wavelength (<100 m) magnetic low directly over the active mound, which was interpreted as a subsurface alteration pipe beneath the active mound or a thermally demagnetized upflow zone. Submersible magnetic profiles, collected over two nearby relict mounds (the *Alvin* and MIR mounds), also found associated magnetization anomaly lows [*Tivey et al.*, 1996] suggesting that crustal alteration rather than thermal demagnetization is the probable cause of these very short-wavelength magnetic lows. Calculations reveal that the short-wavelength magnetization anomalies associated with the TAG active mound and relict mounds cannot be responsible for the broader sea surface magnetic low, indeed, several hundred mounds would be needed to generate the magnitude of the sea surface anomaly [*Tivey et al.*, 1993]. Thus it appears that the sea surface magnetic anomaly low must be generated by another mechanism. One hypothesis is that the magnetization low represents a thermal demagnetization of the crust due a broad thermally active region beneath the TAG hydrothermal field [*Tivey et al.*, 1993]. There is seismic evidence for a dearth of earthquakes beneath the region surrounding the TAG site, as well as a low-velocity zone, suggesting an elevated thermal regime [*Kong et al.*, 1992]. Another hypothesis is that the magnetization low represents thinned magnetic crust due to tectonic extension on a normal fault that forms the eastern valley wall of the TAG segment [*Tivey et al.*, 1993]. We investigate these hypotheses using near-bottom magnetic data collected in 1994 using the deep-towed DSL-120 side scan vehicle [*Kleinrock and Humphris*, 1996]. These intermediate-scale near-bottom data provide

Figure 2. (opposite) (a) Bathymetry map of TAG ridge segment shown in context with adjacent ridge segments. Color change every 100 m. The TAG segment shows no clearly defined axial volcanic ridge (AVR) as is observed on ridge segments to the north or south. Box indicates the region of the 1994 deep-towed side scan and magnetic survey [*Kleinrock and Humphris*, 1996]. Symbol T indicates the location of the TAG active hydrothermal mound. Black outline represents the location of the axial volcanic ridge. (b) Magnetic anomaly map based on sea surface magnetic data (50 nT contour interval). A distinctive magnetic dipole anomaly is located within the Brunhes anomaly over the TAG hydrothermal region with a magnetic high to north and a low to the south. (c) Crustal magnetization map calculated from sea surface magnetic anomaly data for a 0.5 km thick source layer with the upper boundary defined by bathymetry; contour interval is 1 A/m. The TAG segment is marked by a region of low magnetization within the Brunhes anomaly. The TAG active mound is located toward the southern end of this low while relict hydrothermal mounds of the *Alvin* zone are found to the north of the active mound. Magnetization highs are well developed on segments to the south and north and appear centered over the neovolcanic ridge system within the rift valley. For the TAG segment, however, only a weakly defined magnetization high is present toward the western side of the rift valley. (d) Regional tectonic summary map showing segmentation of the TAG region, the location of the axial volcanic ridge system. Normal polarity crust is shaded gray and identified as Brunhes/Matuyama boundary (B/M) and chron 2A. Black areas represent the axial volcanic ridge. The red line is the 3000 m isobath, and the blue line is the 4000 m isobath.

the critical link between the submersible mound-scale surveys and the broad multikilometer-scale sea surface data.

2. TAG Ridge Segment Geologic Setting

[4] The TAG ridge segment is located about halfway between the Kane and Atlantis fracture zones on the MAR ridge (Figure 1) where the ridge segments generally show a right-stepping (eastward stepping) tendency in a northward direction [*Sempere et al.*, 1990; *Tucholke et al.*, 1996]. The rift valleys of each ridge segment are commonly offset by nontransform offsets of less than 30 km [*Sempere et al.*, 1990]. The TAG ridge segment has been extant for at least 20 Myr [*Tucholke et al.*, 1996; *Tivey and Tucholke*, 1998; *Tucholke et al.*, 1998]. The southern offset of the TAG segment has maintained a right-stepping sense and a well-defined character in the bathymetry and gravity and magnetic fields. In contrast, the sense of the northern offset changed ~10 Myr ago from left stepping to right stepping

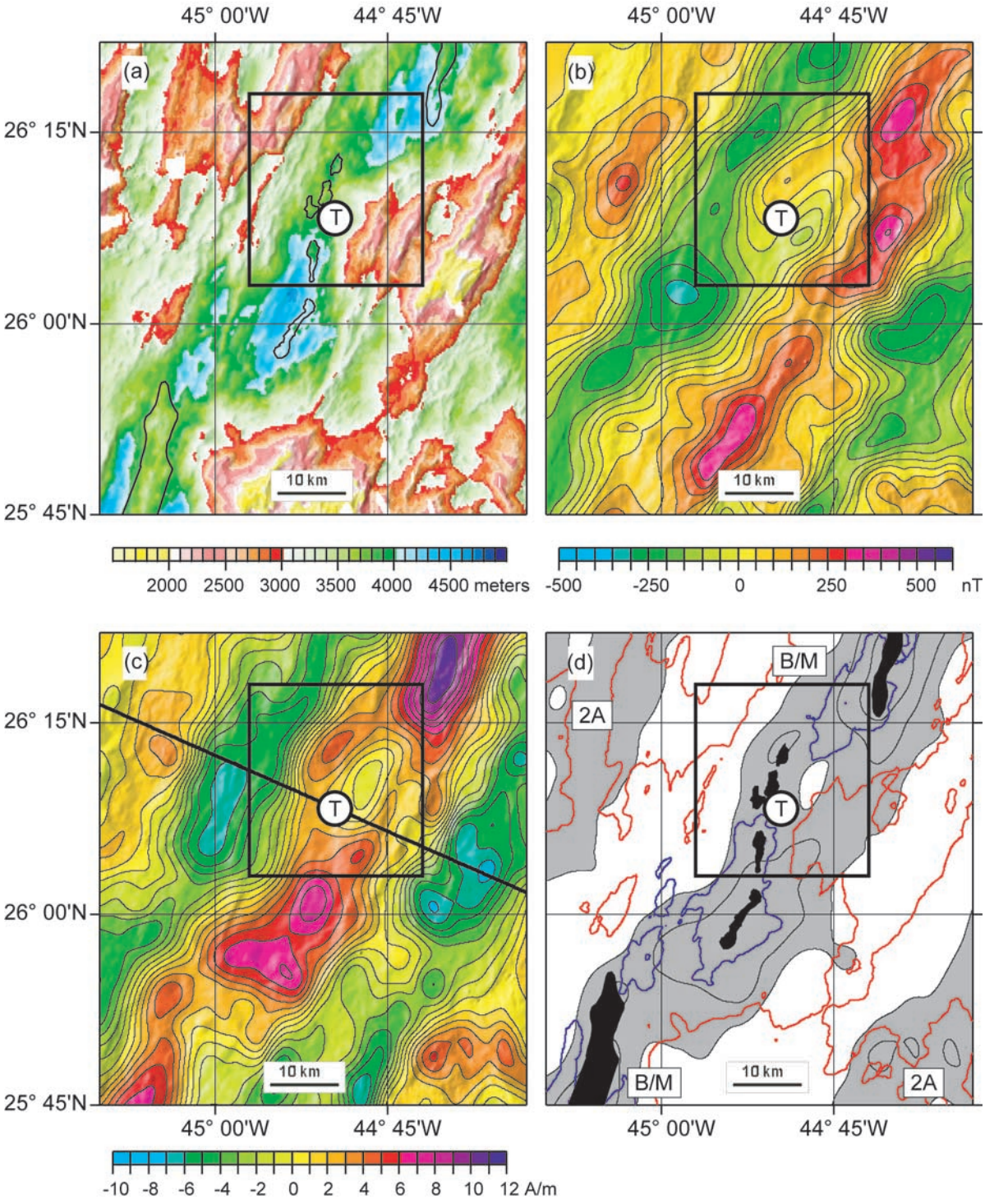

[*Tivey and Tucholke*, 1998]. The present-day TAG ridge segment can be divided into two parts: i.e., north and south of the TAG active mound. The southern half is defined by a strong maximum in crustal magnetization of the Brunhes anomaly (Figure 2c) and an arcuate-shaped axial volcanic ridge that runs along the eastern side of the rift valley deep (Figure 2d). The axial volcanic ridge (AVR) is clearly correlated with the maximum in crustal magnetization of the Brunhes anomaly, which is typically representative of the locus of volcanic accretion (Figures 2c and 2d). The southern end of the AVR terminates at 25°57′N and is separated from the ridge segment to the south by a NNE trending ridge or septum [*Tucholke et al.*, 1996] (Figures 2a and 2d). The northern termination of the AVR is marked by a morphologically distinct volcano [*Kong et al.*, 1992] at 26°05.6′N, 44°51.5′N (Figures 2c and 2d). The northern half of the TAG ridge segment has a weaker maximum in crustal magnetization of the Brunhes anomaly (Figure 2c) and is not as clearly defined. *Kleinrock and Humphris* [1996] identified three small zones of unfissured terrain toward the western side of the rift valley, based on the side scan records from the Deep TAG survey, and interpreted these as being volcanic in origin (Figure 2d). These neovolcanic zones correlate with the sea surface magnetic data, which show a weak magnetization high, asymmetrically positioned toward the western side of the central Brunhes anomaly (Figure 2c). The precise northern termination of the TAG segment remains unclear, but it must step to the right around 26°15′N. By contrast, the ridge segment to the north of the TAG segment is clearly marked by a linear volcanic ridge with a strong magnetization high approximately centered within the Brunhes anomaly (Figures 2c and 2d).

[5] Dominating the central Brunhes anomaly over the northern half of the TAG segment is the sea surface magnetic low, located toward the eastern side of the axial rift valley (Figure 2c). The magnetization low is located near the base of the eastern valley wall, which forms an unusual topographic reentrant into the rift valley of the TAG segment [*Thompson et al.*, 1988], and which is recognized today as an inside corner high [*Tucholke and Lin*, 1994]. Submersible dives by MIR [*Zonenshain et al.*, 1989] and *Alvin* [*Rona et al.*, 1986a; *Karson and Rona*, 1990] found that the eastern wall of this inside corner high is dominated by significant mass wasting and slump materials of basaltic talus and sediments interspersed between steeper escarpments that presumably mark the location of faults. In a number of erosional gullies in the eastern wall, *Zonenshain et al.* [1989] observed a lithological progression from an active mass wasting apron below 3500 m followed by outcropping pillow lava and then a steep scarp that culminates with outcropping altered gabbros and possibly sheeted dikes. Above 2500 m on the uppermost slope are more sediments and debris slide material followed by pillow basalt outcrops. *Karson and Rona* [1990] and *Zonenshain et al.* [1989] attributed the exposure of gabbros and dikes to normal faulting processes requiring >1 km of vertical movement. *Karson and Rona* [1990] interpreted a number of east-west escarpments as representing transfer faults that accommodate movement between various normal fault block systems. They further suggested that hydrothermal activity was localized by the intersection of these transfer zones with normal ridge-parallel zones of faulting and fissuring. On the basis of the 1994 deep-tow side scan survey, however, *Kleinrock and Humphris* [1996] found no direct evidence of this, although they did find a local pattern of intersecting fissure trends that appear to intersect at the TAG active mound [*Bohnenstiehl and Kleinrock*, 2000].

3. Data Collection and Analysis Methods

[6] Near-bottom magnetic field data were collected using a three-axis fluxgate magnetometer mounted to the DSL-120 side-scan sonar fish and towed ~100 m above the seafloor. A total of ~360 km of track lines, spaced ~800 m apart were obtained during the DSL-120 survey [*Kleinrock and Humphris*, 1996]. The survey track lines are shown in Figure 3a and generally run northeast to southwest. Fluxgate magnetometers are not absolute measuring devices and must be calibrated against a reference field and corrected for the magnetic effects of the DSL120 towfish. We used the local value of the regional field based on the IGRF for 1990 extrapolated to 1994 [*IAGA*, 1996] as a reference for the fluxgate magnetic field measurements. The three-axis magnetic component data were then corrected for the effect of the towfish using a best fit coefficient matrix calculated using a least squares solution for the permanent magnetic field of the towfish and singular value decomposition to obtain a minimum norm matrix of coefficients for its induced magnetic field [see *Korenaga*, 1995]. This correction reduced the variation in total field versus towfish orientation from ~15000 nT to less than ~150 nT. The along-track magnetic field and altitude data were sampled onto an equally spaced grid (92 m grid spacing) using a

Figure 3. (opposite) (a) Bathymetry map of the deep-tow survey area showing track lines of DSL-120 vehicle in bold black lines. Contour interval is 100 m. Areas of hydrothermal interest are marked by a T for the TAG active mound, A for *Alvin* relict mound, and M for the relict MIR mound. (b) Magnetic field upward continued to a level plane of 1.9 km below sea level using the algorithm of *Guspi* [1987]. (c) Crustal magnetization computed from the upward continued field and seafloor bathymetry using the *Parker and Huestis* [1974] Fourier inversion method assuming a constant thickness (500 m) source layer. A magnetization high is found to reside over the western side of the rift valley floor while a region of low magnetization appears to coincide with the eastern wall of the rift valley. No obvious discrete magnetic lows appear to correspond directly with the known hydrothermal mounds. (d) Tectonic summary map showing the deep-tow magnetization contour map in color with superimposed contour lines of bathymetry (thin black lines, 100 m contour level) and tectonic elements as interpreted from side scan data. Grey shaded regions represent neovolcanic areas, which correspond with the magnetization high in the deep-tow magnetization inversion. B/M is the sea surface Brunhes-Matuyama reversal boundary and correlates quite well with the deep-tow inversion. A zone of low magnetization corresponds to the eastern rift valley wall. Line of section is the locus of a profile extracted from the map data and shown below.

nearest neighbor algorithm of the GMT software package [*Wessel and Smith*, 1991]. A correction for vehicle altitude above the seafloor was performed by continuing the gridded magnetic field data upward from the uneven observation plane to a level plane at 2.5 km depth using a Fourier transform method [*Guspi*, 1987]. To minimize edge effects, the deep-tow magnetic field data were bordered with sea surface magnetic data that had been downward continued to the level plane at 2.5 km depth. The bordered magnetic field data were then upward continued to 1.9 km depth, which represents the shallowest bathymetry found in the bordered area (Figure 3b). This level is required by the Fourier inversion method to compute crustal magnetization, which assumes all bathy-

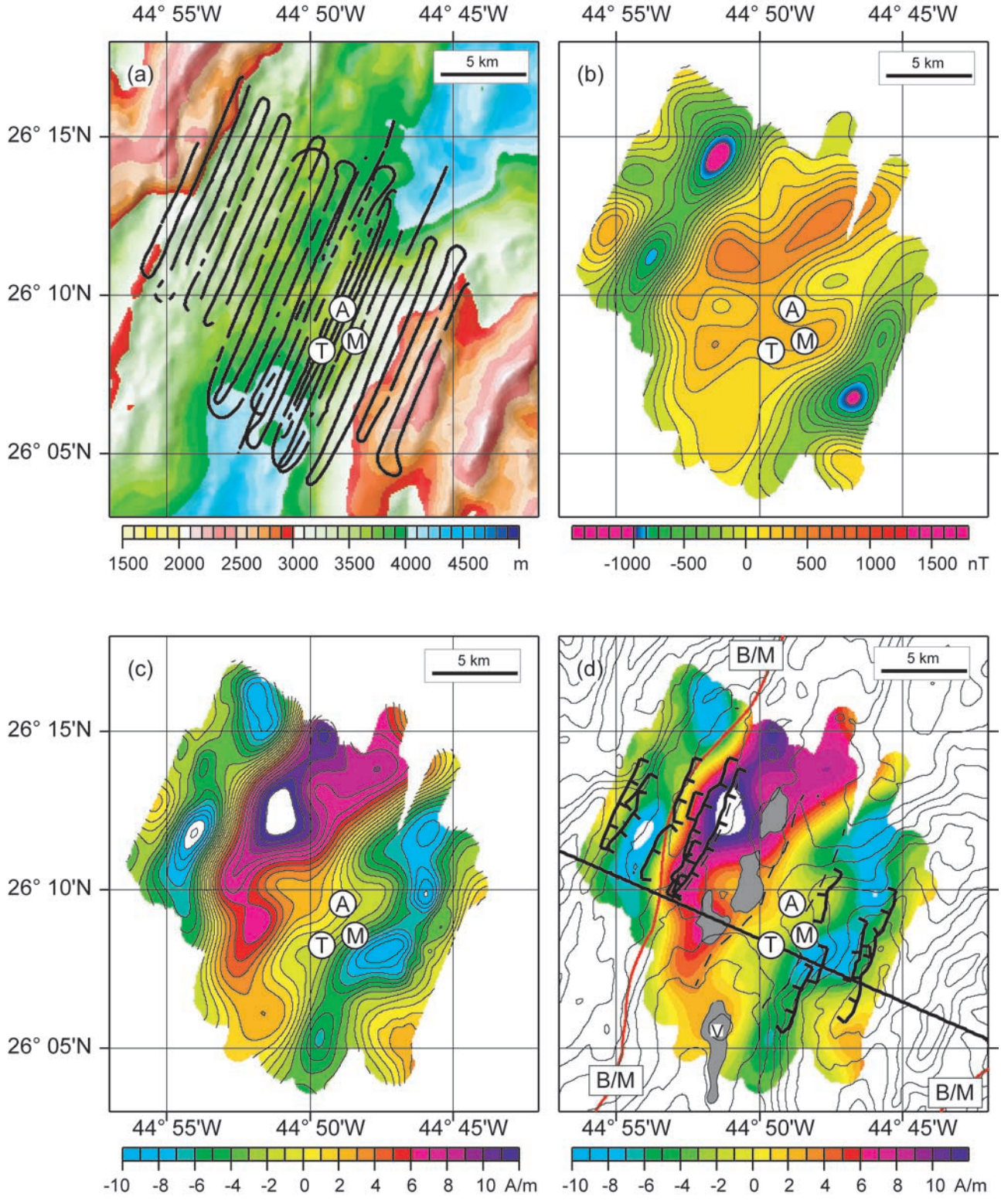

metry lies below the level of observation [*Parker and Huestis*, 1974]. The inversion procedure makes a number of assumptions: a constant thickness source layer (0.5 km) whose upper surface is defined by the bathymetry and a geocentric dipole magnetization direction (i.e., 45° inclination, 0° declination). A band-pass filter with wavelength cutoffs of 47 and 0.5 km and a passband of 23 to 1 km was used to ensure convergence of the solution. The resulting crustal magnetization map is shown in Figure 3c. Inversion is inherently nonunique and one measure of this is the annihilator function, which is a magnetization distribution that when convolved with bathymetry produces no external magnetic field. Thus an infinite amount of annihilator can be added to the solution without affecting the resultant magnetic field. In practice, sufficient annihilator is added to the magnetization solution to balance the positive and reversed polarity amplitudes. The central Brunhes anomaly on the slow spreading MAR typically has higher amplitude than its adjacent anomalies because it is created by young relatively magnetic crust and has constructive enhancement of anomaly sidelobes [*Tivey and Tucholke*, 1998]. Thus a more appropriate method is to balance the amplitude of the chron 2 anomaly to the northwest of the survey area or to look at the width of the Brunhes anomaly. From these approaches it was determined that no annihilator needs to be added to the inversion solution (Figures 3c and 3d).

4. Results and Discussion

[7] The near-bottom magnetic inversion provides information on two main aspects of the geophysical setting of the northern half of the TAG ridge segment: (1) The asymmetrically located zone of high magnetization in the Brunhes anomaly that presumably defines the locus of the neovolcanic axis, and (2) the zone of reduced magnetization in the Brunhes anomaly that generates the strong disturbance in the sea surface magnetic signal over the TAG region.

4.1. Neovolcanic Axis

[8] From the inversion of the near-bottom magnetic data, we find that in the northern half of the TAG segment the strongest magnetization is found near the western edge of the Brunhes anomaly along the westernmost edge of the axial rift valley (Figures 3c and 3d). Typically, the zone of highest magnetization often marks the spreading axis [*Klitgord*, 1976; *Sempere et al.*, 1993]. *Kleinrock and Humphris* [1996] delineated three small zones of unbroken unfissured terrain located within the center and deepest portion of the TAG ridge segment rift valley, which were interpreted as recent, still unfissured volcanic flows (shaded gray in Figure 3d). These zones are located near the eastern edge of the magnetization high. Circular bathymetric features (i.e., individual volcanoes) that lie within the center of the magnetization high can be recognized within the bathymetry data along the westernmost side of the rift valley (Figure 3d). These circular volcanic features are typical of MAR accretion processes [e.g., *Smith and Cann*, 1992], and thus it is speculated that the zone of highest magnetization marks the present neovolcanic axis of the northern half of the TAG segment. Asymmetry in the location of the neovolcanic axis relative to the Brunhes anomaly is also found in other MAR ridge segments (e.g., see the asymmetric location of neovolcanic axes relative to the Brunhes anomaly in the segments directly north and south of the TAG segment (Figure 2c), and notably at 29°N [*Allerton et al.*, 2000] where the sense of asymmetry is opposite to that of the TAG and adjacent segments shown in Figure 2d. The zone of high magnetization in Figures 3c and 3d steps ~3 km eastward at the southern end of the survey area to center over the volcano mentioned by *Kong et al.* [1992], which lies at the northern end of the southern half of the TAG ridge segment (Figures 2d and 3d).

4.2. Zone of Reduced Magnetization

[9] To the east of the magnetization high on the northern half of the TAG segment we find a zone of low magnetization oriented subparallel to the axis of spreading, which is clearly associated with the eastern wall of the axial valley (Figures 3c and 3d). The TAG, MIR and *Alvin* hydrothermal mounds are located on the transition between the magnetization high to the west and the magnetization low to the east and they are clearly not found within the magnetic low itself (Figures 3c and 3d). Thus, as suggested by the submersible magnetic studies of the mounds [*Tivey et al.*, 1993, 1996] and the sea surface magnetic field studies, these hydrothermal systems are not the source of the pronounced magnetic low. The zone of reduced magnetization is, however, clearly located within the Brunhes anomaly, as can be demonstrated by the regional sea surface coverage, cross-axis profiles extracted from the deep-tow and sea surface magnetization inversions and accompanying forward models (see Figures 2c, 3d, and 4). Figure 4 shows the fit of a spreading model compared to an extracted profile taken across the rift valley and the active TAG mound. The model is based on the interval between the sea surface Chron 2A and the Brunhes/Matuyama (B/M) reversal boundaries and has a half-spreading rate of 8.7 ± 0.6 km/Myr to the west and 12.1 ± 0.5 km/Myr to the east (Figure 5). The total opening rate of 20.8 ± 1.1 km/Myr is entirely compatible with previous detailed studies of central MAR plate spreading history [*Sloan and Patriat*, 1992; *Tivey and Tucholke*, 1998]. In the sea surface profiles, the eastern Brunhes/Matuyama boundary is compromised by the overlap of the magnetic end effect of the ridge segment to the north producing an apparently wider Brunhes anomaly (see Figures 2c, 4). The near-bottom data show a close correlation with sea surface data and clearly demonstrate that the zone of reduced magnetization is located well within the Brunhes anomaly (Figure 4). From the near-bottom data, utilizing the B/M and Jaramillo chrons (Figure 6), we estimate a total opening rate of 22 km/Myr (i.e., within the error estimate of 20.8 ± 1.1 km/Myr based on the sea surface data), which we use for the modeling of the profile and calculations of extension. The zone of reduced magnetization averages ~4 km wide with an amplitude contrast of between 15 and 20 A/m for a constant thickness 500 m thick source layer (Figures 4 and 6).

4.3. Source of Reduced Magnetization

[10] The source of reduced magnetization may have occurred when the crust formed and could be geomagnetic in origin either because of reverse polarity or due to

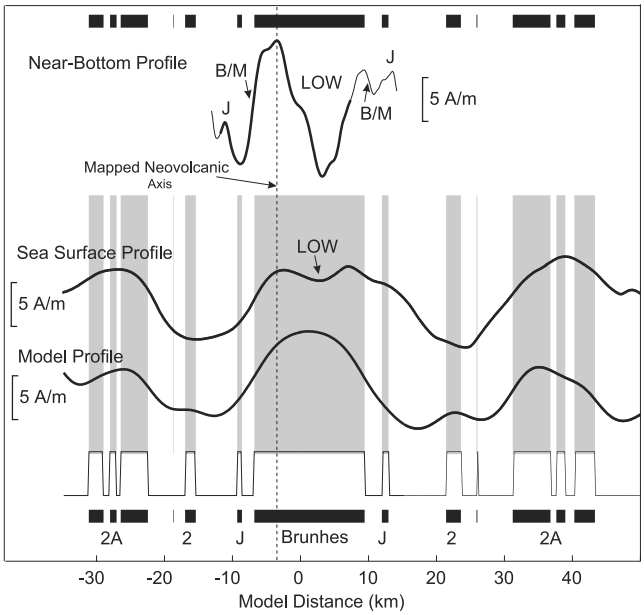

Figure 4. Magnetization profile cross sections taken across the TAG ridge segment from the sea surface (Figure 2c) and deep-tow inversion (Figure 3c). Both profiles show a narrow (~7.5 km) zone of high magnetization located near the western side of the Brunhes anomaly. A zone of low magnetization is located near the center of the Brunhes anomaly overlying the eastern rift valley wall. The bottom plot shows a best fit model using a constant spreading rate of 8.7 km/Myr to the west and 12.1 km/Myr to the east as determined by the analysis shown in Figure 5. The model profile has been Gaussian filtered with a sigma of 1 km and filtered with a low-pass filter with a wavelength cutoff of 3.5 km to simulate the sea surface anomaly result. B/M marks the Brunhes/Matuyama boundary, and J is the Jaramillo. Chron ages are based on the *Cande and Kent* [1995] geomagnetic polarity timescale.

variations in field intensity, or it may reflect crustal accretion processes such as thin volcanic crust due to varying magmatic output. Alternatively, the reduced magnetization could have formed after the crust has be created such as crust demagnetized through mass wasting, thermal demagnetization or alteration, or crust thinned by extensional faulting.

[11] Considering first a geomagnetic origin of the magnetic low, we note that the magnetic low lies within a Brunhes anomaly of the predicted width (Figures 3d and 4), which argues against this being an area of reversed polarity Matuyama crust. Furthermore, the rather normal width of the Brunhes anomaly over the TAG segment and the absence of oblique trends in bathymetry rule out the hypothesis of rift propagation to trap such a zone of reversed polarity. *Kleinrock and Humphris* [1996] envisioned a crustal accretion scenario in which the neovolcanic zone "jumped" westward in order to explain the asymmetrical distribution of fissuring relative to the neovolcanic zone, but this would have occurred within the last 300 kyr and would not have trapped any reversely magnetized crust (Brunhes/Matuyama boundary at 0.78 Ma). Likewise, we also discount the role of geomagnetic paleointensity variation as a possible source of the anomaly because of the slow spreading rate of the MAR and the relatively rapid fluctuations (i.e., thousands of years timescales) seen in the paleointensity record [*Guyodo and Valet*, 1999]. The reduced zone of magnetization is ~4 km wide, which at a total opening rate of 22 km/yr represents a time interval of ~200 kyr. In the most recent published global paleointensity curve [*Guyodo and Valet*, 1999], there is simply no period long enough to generate such a low magnetic zone for such a length of time. For these reasons, we concentrate on the hypotheses that concern crustal accretion and the loss of magnetization either through alteration, thermal demagnetization, mass wasting, or faulting.

[12] Ocean crust undergoes alteration from the moment it is created. Low-temperature oxidation is, however, a gradual process that likely takes place continuously and is typically associated with a long-term loss in amplitude of the magnetic signal [*Bleil and Peterson*, 1983; *Johnson and Pariso*, 1993]. A discrete area of alteration is much more likely to be associated with hydrothermal processes. Hydrothermal alteration can in some instances totally destroy the magnetic signal [e.g., *Rona*, 1978; *Tivey et al.*, 1993; *Tivey and Johnson*, 2002]. However, here at TAG, it is clear that the zones of hydrothermal discharge are not located within the magnetic low zone, but lie at the transition between high and low magnetization, and clearly west of the low magnetization zone. *Tivey et al.* [1993] also pointed out that several hundred mound anomalies would be needed to generate a demagnetization of this magnitude. Thus, while hydrothermal alteration may be important locally, directly beneath the mounds, the mismatch between the location of the hydrothermal mounds and that of the magnetization low suggests that alteration associated with the hydrothermal mounds is not the cause of the magnetic low.

[13] Similarly, we discount thermal demagnetization as a viable source of the magnetization low because of the

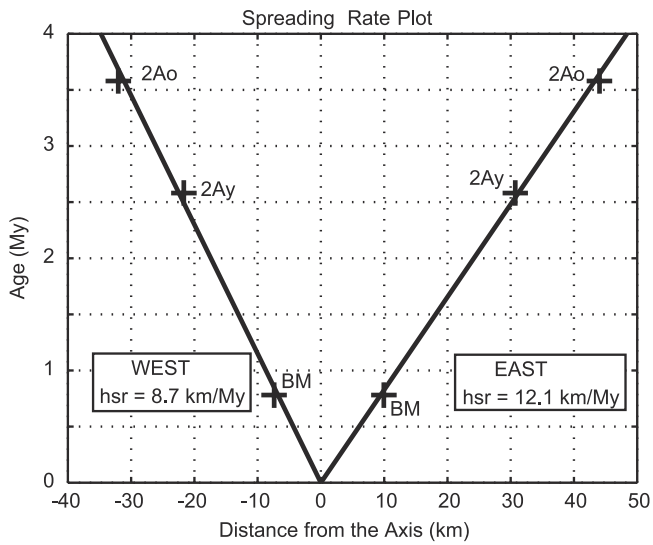

Figure 5. Plot showing the half spreading rates determined from sea surface magnetic data over the TAG region (see Figure 4 for profile). The spreading rates were estimated using a simple linear regression fit to the estimates of magnetic anomaly age and distance.

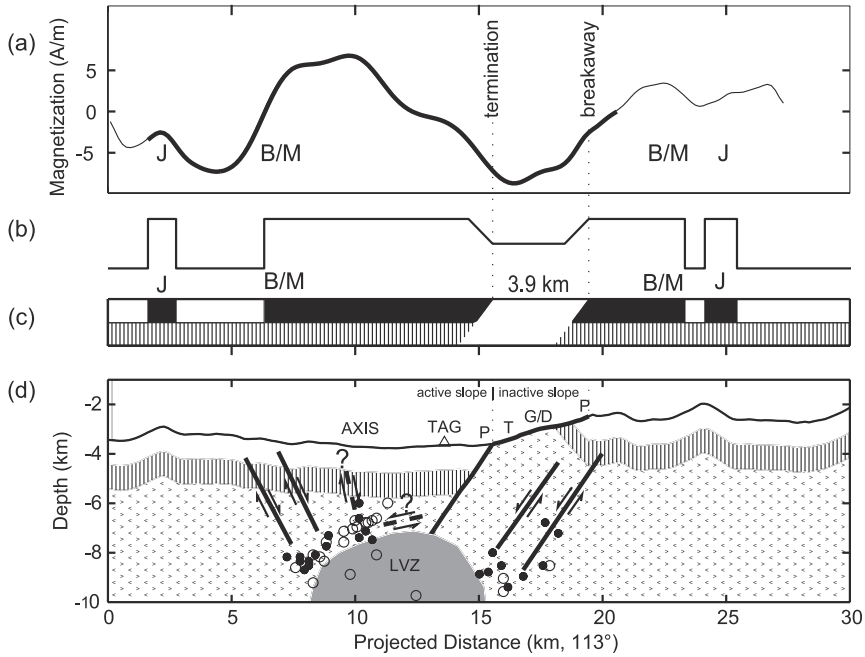

Figure 6. (a) Crustal magnetization profile along line through the TAG mound trending 113° in Figure 3c. Bold part of profile based on the deep-tow data. (b) Reversal timescale model assumes total spreading rate of 22 km/Myr. Zero magnetization matches low in Figure 6a, which is related to normal-fault extension shown below. (c) Model of hanging wall (left) and footwall (right) of a 1km thick magnetic source layer underlain by nonmagnetic sheeted dikes and gabbros cut by a 45° normal fault. Horizontal extension is 3.9 km derived from the width of the low in the crustal magnetization shown in Figure 6a. (d) Cross-section model of extension across the TAG mound area. Bathymetry is from Figure 3a. Hanging wall and footwall in Figure 6c are suspended from bathymetry. Bold line emphasizes active and inactive part of the detachment fault. Other faults, microearthquake hypocenters, slip directions, and low-velocity zone (LVZ) are after *Kong et al.* [1992, Figure 15]. Pillows (P), talus (T), and gabbros and dikes (G/D) on the eastern rift valley wall located at the water depths reported by *Zonenshain et al.* [1989].

mismatch in the location of the low and the hydrothermal vents. It would be expected (although not required) that hydrothermal vents would be located over such a thermally elevated zone. *Kleinrock and Humphris* [1996] and *Tivey et al.* [1993] both hypothesized that the hydrothermal vents at TAG could be underlain by a hot intrusive body that could give rise to a broad magnetic low. The near-bottom magnetic data from this study clearly show, however, that thermal demagnetization is not important at this location and that the observed magnetic low, is in fact located over the eastern valley wall, significantly east of the vent areas. The seismic data of *Kong et al.* [1992] displays a dearth of earthquakes in the region of the hydrothermal mounds, and a low-velocity zone suggesting an intrusive body at several kilometers depth beneath the axis. This seismic structure is clearly not giving rise to any associated magnetic anomaly low (Figure 3). Furthermore, where we do observe a magnetization low, over the eastern wall of the rift valley, the seismic data show a number of deep (~6 km) earthquakes, inferring brittle (i.e., cold) behavior at depth (Figures 3 and 6). Consequently, we think it unlikely that the magnetic low would be caused by any thermal demagnetization effects at this location.

[14] The magnetization low appears to correspond to a zone of major mass wasting [*Karson and Rona*, 1990; *White et al.*, 1998] located on the eastern rift valley wall. Debris slide material will be nonmagnetic due to the random orientation of blocks. If the thickness of mass wasting materials is significant enough, then the magnetization inversion that uses the depth of the seafloor as the top of the source layer would underestimate the effect of the crustal magnetization by assuming a source zone shallower than it actually was. Forward models show that an unreasonable thickness of debris slide material is needed ($\gg$1 km thick) to generate sufficient contrast. Alternatively, mass wasting could have removed the magnetic source at this location. No further observational evidence exists to support the presence of a significantly thick mass wasting deposit [*Zonenshain et al.*, 1989; *Karson and Rona*, 1990].

[15] Crustal accretion at slow spreading ridges like the MAR is not a continuous process. Early work on the process of crustal accretion at the MAR had suggested that variations in the thickness of the extrusive layer could create variability in the resultant magnetic signal [e.g., *Schouten and Denham*, 1979]. The distinctive zone of low magnetization at TAG is not randomly distributed but is located over the lower scarp of the eastern wall of the rift valley and is only found to the east of the axis. Variability in magma supply might cause less crustal material to be accreted and a thinner source layer but this would presumably occur at the axis and thus be recorded on both sides of the spreading center. In this case, the low is only seen east of the axis, and

on the rift valley wall arguing the process is not magmatic in origin. While we cannot rule out variations in the thickness of the source layer due to magmatic accretion the association of the magnetization low with the rift valley wall, the observed faulting and the exposure of gabbros [*Zonenshain et al.*, 1989] suggests that crustal thinning along a single normal fault is the most likely explanation for the magnetization low.

4.4. Missing Source: Extension on a Normal Fault

[16] MIR submersible observations and sampling [*Zonenshain et al.*, 1989] indicate exposures of gabbros and dikes in the eastern rift valley wall of the TAG segment, suggesting the wall is the face of a normal fault with a vertical throw of at least 1 km (Figure 7a) [*Zonenshain et al.*, 1989]. *Zonenshain et al.* [1989] observe an active and an inactive part of the wall that would be equivalent respectively to the hanging wall and footwall of an active normal fault. The location of the actual fault is not known with great accuracy due to doubts about the accuracy of the MIR navigation, which locates the TAG hydrothermal mound 600 meters east of where it presently is thought to be. Note that the location of the TAG active hydrothermal mound based on the 1994 DSL-120A side scan survey is 26°8.252′N 44°49.570′W, which is equivalent to the location published in maps by *White et al.* [1998] and *Humphris and Tivey* [2000]. In Figure 7a, we show our best estimate of the location of the MIR dives and the normal fault relative to the multibeam bathymetry [*Karson and Rona*, 1990] by matching the depth contours and dive descriptions in *Zonenshain et al.* [1989]. Of particular interest is the fault termination proposed by *Zonenshain et al.* [1989], which separates the hanging wall to the west from the footwall to the east (bold fault trace in Figure 7a).

[17] The termination of the normal fault runs slightly west of the axis of the zone of reduced magnetization (Figure 7b). The zone of reduced magnetization appears to closely track the lower part of the exposed footwall. We have modeled this in cross section as shown in Figure 6. The forward modeling shows that extension of the magnetic upper crust along a normal fault at this location would match the magnetic low and expose the appropriate lithologies and extent of footwall as mapped by *Zonenshain et al.* [1989]. Shown in Figure 6 are bathymetry and crustal magnetization along line 1 in Figure 3d, which locates the zone of reduced magnetization between inflection points at km 15.05 and km 18.95. We model the reduced magnetization with a 3.9 km extension of a 1 km thick upper crust magnetic source layer along a ~55° normal fault, which places the fault termination at km 15.55 and the breakaway at km 19.45 (dotted lines in Figure 6). The model termination (western cross on line in Figure 7b), which lies at the slope break, is only 0.6 km west from the location predicted by *Zonenshain et al.* [1989]. The model breakaway (eastern cross on line in Figure 7b) coincides with the scarp at the top of the slope mapped by *Bohnenstiehl and Kleinrock* [2000]. We note here that the magnetic modeling is relatively insensitive to the dip of the fault, at least for faults dipping between 30 and 60 degrees, and the lateral difference would be small compared to the error (~1 km) in picking the inflection points of the anomaly.

[18] The 3.9 km of horizontal extension along a ~55° normal fault exhumes ~3.2 km of upper oceanic crust, or, more than enough to expose gabbros and dikes on the inactive fault face of the footwall. The approximate location of outcrops of gabbros (G) and dikes (D) reported by *Zonenshain et al.* [1989] are indicated at the appropriate depths of the seafloor in Figure 6 where they show a strong correspondence to the proposed model.

[19] Results of a bottom seismometer survey [*Kong et al.*, 1992, Figure 15] are also plotted in Figure 6. Solid and open circles shown in Figure 6 represent microearthquake hypocenters projected on a vertical plane through the TAG mound location with an azimuth of 110°, or, only 3° less than the azimuth of line 1, which also runs through the TAG mound location (see Figure 6). Focal mechanism solutions derived from these microearthquakes (Figure 6) indicate normal faulting activity dipping ~55°NW in the deeper cluster ~7 km east of the axis, and dipping up to 80°SE in the shallower cluster immediately west of the axis. We propose the deeper earthquakes east of the axis are related to the amagmatic extension and uplift in the eastern rift valley wall, whereas the shallower activity immediately west of the axis relates to near-vertical collapse of the rift valley inner floor at the magmatic axis. The low-velocity zone (LVZ in Figure 6) mapped by *Kong et al.* [1992] is symmetrically located between the magmatic axis and the locus of amagmatic extension represented by the proposed fault.

4.5. Implications for the Causes of Long-Lasting Hydrothermal Systems

[20] The horizontal extension of 3.9 km, estimated from the width of the zone of reduced magnetization, is in agreement with the exhumation of gabbros and dikes along a single normal fault (Figure 6). This fault forms the eastern wall of an inside corner high that is associated with the northern right stepping offset of the TAG segment. The fault lies ~4 km inside the Brunhes/Matuyama boundary (0.78 Ma) and must therefore be less than ~0.5 Myr old. The *Zonenshain et al.* [1989] observations of an active hanging wall and an inactive footwall suggest the fault is still active. The cluster of microearthquakes below the footwall in Figure 6 suggests the same. The minimum age of the fault is ~175 kyr (i.e., 3.9 km/22 km/Myr) assuming all spreading was taken up by amagmatic extension on the fault. We estimate, therefore, that the fault has been active since 0.35 ± 0.1 Ma. The estimated age of the fault and its present offset represent a mean horizontal slip rate of ~11 km/Myr, or, half the total spreading rate of 22 km/Myr. This implies magmatic extension of only ~11 km/Myr at the neovolcanic axis during the past 0.35 Myr. This low magmatic extension rate may account for the lack of a robust AVR in the northern half of the TAG segment compared with the AVR's in the southern half of the segment and in the segments north and south.

[21] A fault that slips 1 m/100 years over several hundred thousand years predicts earthquake activity episodically disturbing the hanging wall on which the active TAG mound and nearby relict hydrothermal mounds are located. Since all the hydrothermal mounds are located on the hanging wall, they were always in the same relation to the active fault, maintaining a constant distance of less than 3 km from the fault (Figures 6 and 8). We propose that over

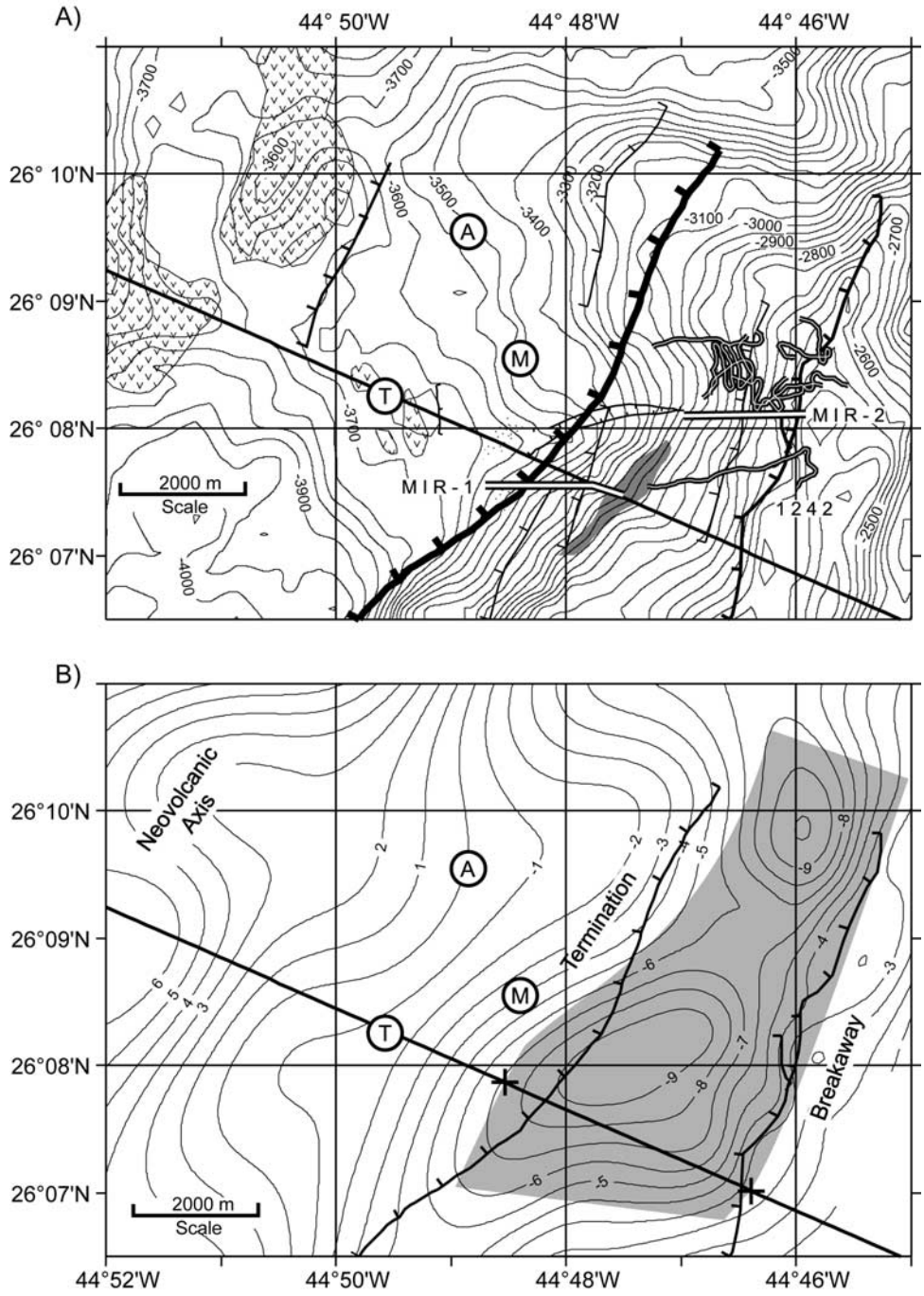

Figure 7. (a) Detailed bathymetry map of the TAG area (contour interval of 50 m) showing the location of the MIR dives (MIR-1 and MIR-2) and observations from *Zonenshain et al.* [1989] and the *Alvin* dives (bold lines with central white stripe) of *Karson and Rona* [1990]. Shaded gray zone marks the occurrence of gabbro outcrop; the area of v's represents volcanics and the neovolcanic zone as mapped by *Kleinrock and Humphris* [1996]. Faults with hachure marks are from *Kleinrock and Humphris* [1996], and the bold line with hachures is the main rift valley normal fault from *Zonenshain et al.* [1989]. T marks the location of the TAG active mound, M the MIR mound, and A the *Alvin* mound. West to east line marks the location of the cross section extracted from the data (Figures 4 and 6). (b) Magnetization contours (contour interval of 1 A/m) from near-bottom data (Figure 3c) showing the correlation of the magnetization low with the location of the footwall exposure and fault zone location (bold lines with hachures from Figure 7a). Gray shading, based on the near-bottom magnetic data, marks the predicted exposure of upper crust between the termination and breakaway limits of the proposed normal fault. Crosses mark these limits shown in the cross section of Figure 6.

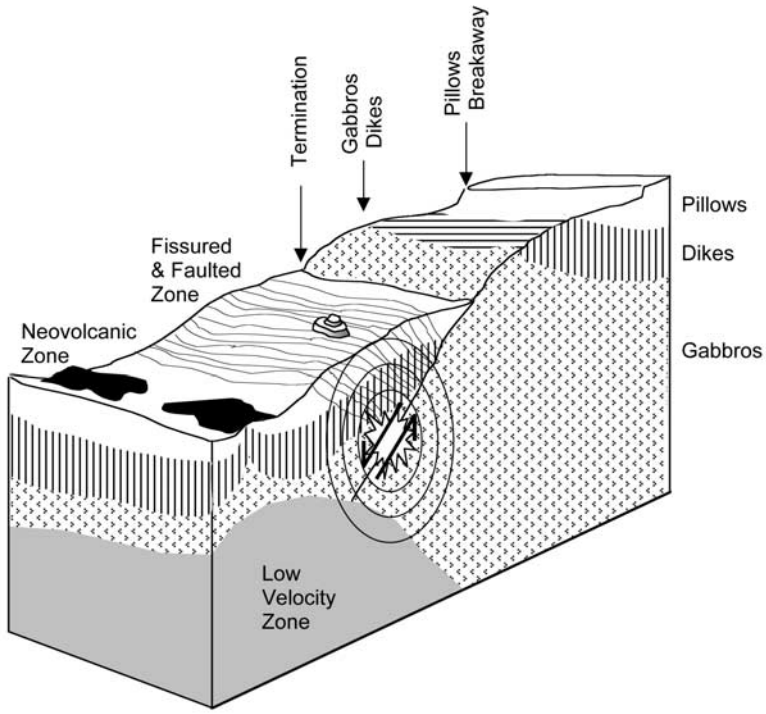

Figure 8. Cartoon of the eastern half of the TAG rift valley. A long-lived fault exhumes pillows, dikes and gabbros exposed between breakaway and termination on the eastern wall of the valley. Over the past several hundred thousand years, continued movement on the fault has deformed the hanging wall in the fissured and faulted zone and episodically increased its permeability enabling seawater to revitalize the active TAG mound and the other nearby hydrothermal circulation systems. Note that TAG, MIR, and *Alvin* hydrothermal systems are located in the hanging wall, which maintains a constant relation to the active part of the fault.

the past several hundred thousand years, movement on the normal fault has episodically increased the permeability of the hanging wall enabling seawater to restart the active TAG mound and the other hydrothermal circulation systems (Figure 8). Evidence for repeated cycles of vigorous hydrothermal activity based on radionucleide isotope studies have been reported by *Lalou et al.* [1995] and *You and Bickle* [1998], who find ~2000 year episodicity over the past 20 kyr and possibly longer [*Humphris and Tivey*, 2000]. The other mounds in the TAG area, such as the MIR and *Alvin* mounds, have variously older dates up to 140 kyr [see *Humphris and Tivey*, 2000, and references therein].

[22] *Bohnenstiehl and Kleinrock* [2000] documented a zone of fissuring that encompasses the TAG hydrothermal field and alternatively suggest that dike intrusion is the primary mechanism for the creation of this fissured zone and for the increased permeability needed for hydrothermal flow. *Humphris and Tivey* [2000] suggested that the episodic history of the TAG hydrothermal area is controlled by the large-scale faulting associated with the formation of the eastern rift valley wall and that either episodic magmatism or the occurrence of faulting was driving the pattern of hydrothermal activity at TAG. From our magnetic analysis, we provide clear evidence and more strongly assert that it is the normal faulting activity that appears to be the major driving force behind the ongoing hydrothermal activity at TAG rather than the magmatic activity. We further speculate that significant hydrothermal deposits like TAG may be typically associated with hanging walls of long-term detachment faults near seafloor spreading centers. This would imply that it is not so much the injection of heat from below as the reactivated permeability of the crust related to repeated movement on a detachment fault that controls long-term behavior and longevity of such hydrothermal systems (Figure 8).

5. Conclusions

[23] We believe the magnetization low in the northern half of the TAG segment is not caused by alteration related to the TAG nearby hydrothermal systems, but by crustal thinning along a normal fault that forms the wall of an inside corner high. We have constructed a model that satisfies most of the observations. Geomagnetic causes can be ruled out due to the location and longevity of the magnetic low. The magnetic low is located over the eastern rift valley wall and clearly west of the hydrothermal fields. The microearthquake data show a dearth of earthquakes beneath the TAG hydrothermal region but brittle faulting beneath the magnetic low and eastern wall suggesting that thermal demagnetization is not important in generating a magnetic low. Submersible and side scan observations of the eastern wall show a faulting geometry that leads to exposure of lower crust, which corresponds to the location of the magnetic low. The combination of these observations therefore leads us to the conclusions that the magnetic low

is caused by structural thinning rather than magmatic thinning. The estimated horizontal extension on the fault is 3.9 km, which is sufficient to exhume the dikes and gabbros observed and sampled on the eastern rift valley wall. The fault is still active. The minimum age of the fault would be 175 kyr (i.e., 3.9 km/22 km/Myr) if no axial magmatic extension had been occurring during that time. A more reasonable estimate is that the age of the fault is ~350 ± 100 kyr, which implies that half of the 22 km/Myr spreading rate was taken up by magmatic extension at the axis, and the remaining half by amagmatic extension along the fault. Long-term simultaneous extension at the axis and along a fault located 13 km to the east would explain the asymmetrical location of the magmatic axis relative to the Brunhes anomaly.

[24] TAG and the other hydrothermal systems are located on the hanging wall of a long-term detachment fault. We propose that over the past several hundred thousand years, movement on the fault has episodically increased the permeability of the hanging wall enabling seawater to revitalize the active TAG mound and the other nearby hydrothermal circulation systems. We speculate that significant hydrothermal deposits like TAG may be typically associated with hanging walls of long-term detachment faults near seafloor spreading centers. This would imply that it is not so much the injection of heat from below as the reactivation of permeable fluid pathways within the crust related to repeated movement on the detachment fault that controls the longevity of such hydrothermal systems.

[25] **Acknowledgments.** We thank the members of the Deep Submergence Group at Woods Hole Oceanographic Institution for their efforts in collecting the original data. Maurice Tivey and Hans Schouten thank Susan Humphris, Peter Rona, and Meg Tivey for encouragement and discussion during the writing of this paper. Martin Kleinrock thanks Del Bohnenstiehl, Sheri White, Mamum Rashid, and Julia Getsiv. The authors thank reviewers Graham Kent, an anonymous reviewer and Associate Editor and the Editor Francis Albarede for their comments on an earlier version of this paper.

References

Allerton, S., J. Escartin, and R. C. Searle, Extremely asymmetric magmatic accretion of oceanic crust at the ends of slow-spreading ridge segments, *Geology*, *28*, 179–182, 2000.

Bleil, U., and N. Peterson, Variations in magnetization intensity and low-temperature titanomagnetite oxidation of ocean floor basalts, *Nature*, *301*, 384–388, 1983.

Bohnenstiehl, D. R., and M. C. Kleinrock, Fissuring near the TAG active hydrothermal mound, 26°N on the Mid-Atlantic Ridge, *J. Volcanol. Geotherm. Res.*, *98*, 33–48, 2000.

Cande, S. C., and D. V. Kent, Revised calibration of the geomagnetic polarity timescale for the late Cretaceous and Cenozoic, *J. Geophys. Res.*, *100*, 6093–6095, 1995.

Guspi, F., Frequency-Domain reduction of potential field measurements to a horizontal plane, *Geoexploration*, *24*, 87–98, 1987.

Guyodo, Y., and J.-P. Valet, Global changes in intensity of the Earth's magnetic field during the past 800 kyr, *Nature*, *399*, 249–252, 1999.

Humphris, S. E., and M. K. Tivey, A synthesis of geological and geochemical investigations of the TAG hydrothermal field: Insights into fluid flow and mixing processes in a hydrothermal system, in *Ophiolites and Oceanic Crust: New Insights From Field Studies in the Ocean Drilling Program*, edited by Y. Dilek et al., *Spec. Pap. Geol. Soc. Am.*, *349*, 213–235, 2000.

International Association of Geomagnetism and Aeronomy (IAGA), Division V, Working Group 8, International Geomagnetic Reference Field, revision 1995, *Geophys. J. Int*, *125*, 318–321, 1996.

Johnson, H. P., and J. E. Pariso, Variations in oceanic crustal magnetization: Systematic changes in the last 160 million years, *J. Geophys. Res.*, *98*, 435–446, 1993.

Karson, J. A., and P. A. Rona, Block-tilting, transfer faults, and structural control of magmatic and hydrothermal processes in the TAG area, Mid-Atlantic Ridge 26°N, *Geol. Soc. Am. Bull.*, *102*, 1635–1645, 1990.

Kleinrock, M. C., and S. E. Humphris, Structural controls on the localization of seafloor hydrothermal activity at the TAG active mound, Mid-Atlantic Ridge, *Nature*, *382*, 149–153, 1996.

Klitgord, K. D., Sea-floor spreading: The central anomaly magnetization high, *Earth Planet. Sci. Lett.*, *29*, 201–209, 1976.

Kong, L. S., S. C. Solomon, and G. M. Purdy, Microearthquake characteristics of a mid-ocean ridge along-axis high, *J. Geophys. Res.*, *97*, 1659–1685, 1992.

Korenaga, J., Comprehensive analysis of marine magnetic vector anomalies, *J. Geophys. Res.*, *100*, 365–378, 1995.

Lalou, C., J.-L. Reyss, E. Brichet, P. A. Rona, and G. Thompson, Hydrothermal activity on a 10^5-year scale at a slow-spreading ridge, TAG hydrothermal field, Mid-Atlantic Ridge 26°N, *J. Geophys. Res.*, *100*, 17,855–17,862, 1995.

Lisitsyn, A. P., Y. A. Bogdanov, L. P. Zonenshayn, M. I. Kuz'min, and A. M. Sagalevich, Hydrothermal phenomena in the Mid-Atlantic Ridge at lat. 26°N (TAG hydrothermal field), *Int. Geol. Rev.*, *31*, 1183–1198, 1989.

Macdonald, K. C., S. P. Miller, S. P. Huestis, and F. N. Spiess, Three-dimensional modeling of a magnetic reversal boundary from inversion of deep-tow measurements, *J. Geophys. Res.*, *85*, 3670–3680, 1980.

McGregor, B. A., C. G. A. Harrison, J. W. Lavelle, and P. A. Rona, Magnetic anomaly pattern on the Mid-Atlantic Ridge crest at 26°N, *J. Geophys. Res.*, *82*, 231–238, 1977.

Parker, R. L., and S. P. Huestis, The inversion of magnetic anomalies in the presence of topography, *J. Geophys. Res.*, *79*, 1587–1594, 1974.

Purdy, G. M., H. Schouten, M. A. Tivey, and J.-C. Sempere, High-resolution central magnetic anomaly field along the Mid-Atlantic Ridge between 24°N and 31°N, *Eos Trans. AGU*, *70*, 468, 1989.

Rona, P. A., *Marine Geology: The Trans-Atlantic Geotraverse*, pp. 252–256, McGraw-Hill, New York, 1973.

Rona, P. A., Magnetic signatures of hydrothermal alteration and volcanogenic mineral deposits in oceanic crust, *J. Volcanol. Geotherm. Res.*, *3*, 219, 1978.

Rona, P. A., R. N. Harbison, B. G. Bassinger, R. B. Scott, and A. J. Nalwalk, Tectonic fabric and hydrothermal activity of Mid-Atlantic Ridge crest (lat 26°N), *Geol. Soc. Am. Bull.*, *87*, 661–674, 1976.

Rona, P. A., G. Thompson, M. J. Mottl, J. A. Karson, W. J. Jenkins, D. Graham, M. Mallette, J. Von Damm, and J. M. Edmond, Hydrothermal activity at the TAG hydrothermal field, Mid-Atlantic Ridge crest at 26°N, *J. Geophys. Res.*, *89*, 1365–1377, 1984.

Rona, P. A., G. Klinkhammer, T. A. Nelsen, J. H. Trefry, and H. Elderfield, Black smokers, massive sulphides and vent biota at the Mid-Atlantic Ridge, *Nature*, *321*, 33–37, 1986a.

Rona, P. A., R. A. Pockalny, and G. Thompson, Geologic setting and heat transfer of black smokers at the TAG hydrothermal field, *Eos Trans. AGU*, *67*, 1021, 1986b.

Rona, P. A., Y. A. Bogdanov, E. G. Gurvich, A. Rimski-Korsakov, A. M. Sagalevitch, M. D. Hannington, and G. Thompson, Relict hydrothermal zones in the TAG hydrothermal field, Mid-Atlantic Ridge 26°N, 45°W, *J. Geophys. Res.*, *98*, 9715–9730, 1993a.

Rona, P. A., M. D. Hannington, C. V. Raman, G. Thompson, M. K. Tivey, S. E. Humphris, C. Lalou, and S. Petersen, Active and relict seafloor hydrothermal mineralization at the TAG hydrothermal field, Mid-Atlantic Ridge, *Econ. Geol.*, *18*, 1989–2017, 1993b.

Schouten, H., and C. R. Denham, Modeling the oceanic magnetic source layer, in *Deep Sea Drilling Results in the Atlantic Ocean: Ocean Crust*, *Maurice Ewing Ser.*, vol. 2, edited by M. Talwani, C. G. A. Harrison, and D. E. Hayes, pp. 151–159, AGU, Washington, D. C., 1979.

Scott, M. R., R. B. Scott, P. A. Rona, L. W. Butler, and A. J. Nalwalk, Rapidly accumulating manganese deposit from the median valley of the Mid-Atlantic Ridge, *Geophys. Res. Lett.*, *1*, 355–358, 1974a.

Scott, S. D., P. A. Rona, B. A. McGregor, and M. R. Scott, The TAG hydrothermal field, *Nature*, *251*, 301, 1974b.

Sempere, J.-C., G. M. Purdy, and H. Schouten, Segmentation of the Mid-Atlantic Ridge between 24°N and 30°40′N, *Nature*, *344*, 427–431, 1990.

Sempere, J.-C., J. Lin, H. S. Brown, H. Schouten, and G. M. Purdy, Segmentation and morphotectonic variations along a slow-spreading center: The Mid-Atlantic Ridge (24°00′N–30°40′N), *Mar. Geophys. Res.*, *15*, 153–200, 1993.

Sloan, H., and P. Patriat, Kinematics of the North American-African plate boundary between 28° and 29°N during the last 10 Ma: Evolution of the axial geometry and spreading rate and direction, *Earth Planet. Sci. Lett.*, *113*, 323–341, 1992.

Smith, D. K., and J. R. Cann, The role of seamount volcanism in crustal construction at the Mid-Atlantic Ridge (24°–30°N), *J. Geophys. Res.*, *97*, 1645–1658, 1992.

Thompson, G., M. J. Mottl, and P. A. Rona, Morphology, mineralogy, and chemistry of hydrothermal deposits from the TAG area, 26°N Mid-Atlantic Ridge, *Chem. Geol.*, *49*, 243–257, 1985.

Thompson, G., S. E. Humphris, B. Schroeder, M. Sulanowska, and P. A. Rona, Active vents and massive sulfides at 26°N (TAG) and 23°N (Snake Pit) on the Mid-Atlantic Ridge, *Can. Mineral.*, *26*, 697–711, 1988.

Tivey, M. A., and H. P. Johnson, Crustal magnetization reveals subsurface structure of Juan de Fuca Ridge hydrothermal vent fields, *Geology*, *30*, 979–982, 2002.

Tivey, M. A., and B. E. Tucholke, Magnetization of oceanic crust from 0 to 29 Ma formed at the Mid-Atlantic Ridge 25°30′ to 27°10′N, *J. Geophys. Res.*, *103*, 17,807–17,826, 1998.

Tivey, M. A., P. A. Rona, and H. Schouten, Reduced crustal magnetization beneath the active sulfide mound, TAG hydrothermal field, Mid-Atlantic Ridge 26°N, *Earth Planet. Sci. Lett.*, *115*, 101–115, 1993.

Tivey, M. A., P. A. Rona, and M. C. Kleinrock, Reduced crustal magnetization beneath relict hydrothermal mounds of the TAG hydrothermal field, Mid-Atlantic Ridge, 26°N, *Geophys. Res. Lett.*, *23*, 3511–3514, 1996.

Tucholke, B. E., and J. Lin, A geological model for the structure of ridge segments in slow spreading ocean crust, *J. Geophys. Res.*, *99*, 1937–1958, 1994.

Tucholke, B. E., J. Lin, M. C. Kleinrock, M. A. Tivey, T. Reed, J. Goff, and G. E. Jaroslow, Segmentation and crustal structure of the western Mid-Atlantic Ridge flank, 25°30′–27°10′ and 0–29 M. Y., *J. Geophys. Res.*, *102*, 10,203–10,223, 1996.

Tucholke, B. E., K. Fuijoka, and T. Ishihara, Shinkai 6500 dives on Dantes Domes, a megamullion in the eastern rift mountains of the Mid-Atlantic Ridge at 26. 6°N, *Eos Trans. AGU*, *79*(45), Fall Meet. Suppl., F45, 1998.

Wessel, P., and W. H. Smith, Free software helps map and display data, *Eos Trans. AGU*, *72*, 441, 445–446, 1991.

White, S. N., S. E. Humphris, and M. C. Kleinrock, New observations on the distribution of past and present hydrothermal activity in the TAG area of the Mid-Atlantic Ridge, *Mar. Geophys. Res.*, *20*, 41–56, 1998.

Wooldridge, A. L., S. E. Haggerty, P. A. Rona, and G. A. Harrison, Magnetic properties and opaque mineralogy of rocks from selected seafloor hydrothermal sites at oceanic ridges, *J. Geophys. Res.*, *95*, 12,351–12,374, 1990.

Wooldridge, A. L., C. G. A. Harrison, M. A. Tivey, P. A. Rona, and H. Schouten, Magnetic modeling near selected areas of hydrothermal activity on the Mid-Atlantic and Gorda Ridges, *J. Geophys. Res.*, *97*, 10,911–10,926, 1992.

You, C.-F., and M. J. Bickle, Evolution of an active sea-floor massive sulfide deposit, *Nature*, *394*, 668–672, 1998.

Zonenshain, L. P., M. I. Kuzmin, A. P. Lisitsin, Y. A. Bogdanov, and B. V. Baranov, Tectonics of the Mid-Atlantic rift valley between the TAG and MARK areas (26–24°N): Evidence for vertical tectonism, *Tectonophysics*, *159*, 1–23, 1989.

M. C. Kleinrock, Department of Geology, Vanderbilt University, Box 1805 Station B, Nashville, TN 37235, USA. (martykleinrock@yahoo.com)

H. Schouten and M. A. Tivey, Department of Geology and Geophysics, Woods Hole Oceanographic Institution, 360 Woods Hole Road, Woods Hole, MA 02543-1542, USA. (mtivey@whoi.edu)